ROYAL SOCIETY OPEN SCIENCE

rsos.royalsocietypublishing.org

Research

Cite this article: Park J, Mun J, Shin J-S, Kang S-W. 2018 Highly sensitive two-dimensional MoS_2 gas sensor decorated with Pt nanoparticles. *R. Soc. open sci.* **5**: 181462.
http://dx.doi.org/10.1098/rsos.181462

Received: 26 September 2018
Accepted: 6 November 2018

Subject Category:
Chemistry

Subject Areas:
environmental chemistry

Keywords:
molybdenum disulfide, transition metal dichalcogenides, gas sensor, Pt nanoparticles

Author for correspondence:
Sang-Woo Kang
e-mail: swkang@kriss.re

This article has been edited by the Royal Society of Chemistry, including the commissioning, peer review process and editorial aspects up to the point of acceptance.

†These authors contributed equally to the study.

THE ROYAL SOCIETY PUBLISHING

Highly sensitive two-dimensional MoS_2 gas sensor decorated with Pt nanoparticles

Jaeseo Park[1,2,†], Jihun Mun[1,†], Jae-Soo Shin[3] and Sang-Woo Kang[1,2]

[1]Advanced Instrumentation Institute, Korea Research Institute of Standards and Science, Daejeon 34113, Republic of Korea
[2]Science of Measurement, University of Science and Technology, Daejeon 34113, Republic of Korea
[3]Department of Advanced Materials Engineering, Daejeon University, Daejeon 34520, Republic of Korea

S-WK, 0000-0001-5245-0300

A two-dimensional molybdenum disulfide (MoS_2)-based gas sensor was decorated with Pt nanoparticles (NPs) for high sensitivity and low limit of detection (LOD) for specific gases (NH_3 and H_2S). The two-dimensional MoS_2 film was grown at 400°C using metal organic gas vapour deposition. To fabricate the MoS_2 gas sensor, an interdigitated Au/Ti electrode was deposited using the electron beam (e-beam) evaporation method with a stencil mask. The MoS_2 gas sensor without metal decoration sensitively detects NH_3 and H_2S gas down to 2.5 and 30 ppm, respectively, at room temperature (RT). However, for improved detection of NH_3 and H_2S gas, we investigated the functionalization strategy using metal decoration. Pt NP decoration modulated the electronic properties of MoS_2, significantly improving the sensitivity of NH_3 and H_2S gas by 5.58× and 4.25×, respectively, compared with the undecorated MoS_2 gas sensor under concentrations of 70 ppm. Furthermore, the Pt NP-decorated MoS_2 sensor had lower LODs for NH_3 and H_2S gas of 130 ppb and 5 ppm, respectively, at RT.

1. Introduction

Metal oxide-based gas sensors possess many merits, such as relatively high sensitivity and low cost, which has garnered much attention to the material [1]. However, to obtain such gas-sensing properties for a specific gas, these gas sensors generally suffer from several issues, such as thermal instability and high power consumption, due to poor performance at low operating temperatures [1]. As gas detection relies strongly on the properties

of material, new materials that possess excellent characteristics for adsorption of gas molecules at low operating temperatures are in great demand as a way to overcome these deficiencies.

Among the new sensing materials, the two-dimensional materials [2–22] with novel and unique electronic, optical and mechanical properties have attracted much attention. In addition to their excellent properties, the novel two-dimensional gas-sensing materials possess structural advantages, such as a high surface-to-volume ratio and the tunable functionality of the surface for decoration species or functional groups, so they have attracted immense interest as new gas-sensing materials [2–4] that can sensitively react upon exposure to a lower level of a specific gas at low temperature. Even though graphene [5–7]—with its outstanding characteristics—is the most widely known two-dimensional material, transition metal dichalcogenides (TMDCs) [8–13,15–22] have great potential to serve as new materials for advanced electronic devices owing to their excellent characteristics, such as high electron mobility, high flexibility, high elasticity and low power consumption. The charge transfer mechanism between gas molecules and molybdenum disulfide (MoS_2)—which is a typically known two-dimensional TMDC—was previously reported for gas detection [15]. In addition, to improve the performance of the gas sensor, various studies on functionalization using metal [23–30] or metal oxide [31,32] and structural modification [17,33] have been reported. Especially, functionalization [23–32] using metal decoration [23–30] on two-dimensional materials can open an avenue for gas detection [23–32].

In this work, we investigated the performance of a two-dimensional MoS_2-based gas sensor and the effects of functionalization using Pt nanoparticle (NP) decoration. Metal organic chemical vapour deposition (MOCVD), which can control the number of two-dimensional material layers and synthesize scalable two-dimensional-layered materials with high quality, was employed to grow the two-dimensional MoS_2 film. Moreover, MOCVD is capable of synthesizing high-quality two-dimensional MoS_2 directly on the sensor substrate to easily fabricate the MoS_2 gas sensor. The MoS_2 sensor consisted of the MOCVD-grown MoS_2 film as the active channel and an interdigitated Au/Ti electrode fabricated using the electron beam (e-beam) evaporation method with a stencil mask. At room temperature (RT), the MoS_2 sensor could sensitively detect down to 2.5 and 30 ppm for NH_3 and H_2S gas, respectively. However, the detection of NH_3 and H_2S gas still requires higher sensitivity and a lower limit of detection (LOD) owing to the inhalation toxicology of both gases.

Because both gases exhibit inhalation toxicology that leads to lung and organ injury or even death as well as skin irritation, several international standards have been developed as guidelines to assist in the control of these health hazards. For example, the permissible exposure limits, i.e. regulatory limits, in the work place stipulated by the Occupational Safety and Health Administration (OSHA) are 50 ppm for NH_3 and 10 ppm for H_2S. However, in many cases, the recommended limits of NH_3 and H_2S gas, which are characterized by an extremely irritating odour, lie below the regulatory limit stipulated by OSHA, so studies for high sensitivity and low LOD are still required. Thus, we investigated a functionalization strategy, i.e. metal decoration, to obtain excellent gas-sensing characteristics (e.g. higher sensitivity and lower LOD) for NH_3 and H_2S gas. To improve the sensitivity and LOD for NH_3 and H_2S gas, which act as electron donors on the MoS_2, Pt metal NPs, which resist corrosion and oxidation, yielding stable doping as a noble metal [27], are used as the decorating material. Furthermore, Pt NPs double the p-type doping effect compared with Au NPs [27], which commonly act as a p-dopant [12], so Pt NPs could improve the sensing characteristics for NH_3 and H_2S gas. Even though various studies have already been reported [15–19,34] on the detection of various toxic gases (e.g. NO_2, NH_3, H_2 and CO_2) using two-dimensional TMDC-based sensors, most use flake or bulk two-dimensional TMDC instead of two-dimensional MoS_2 film at RT. In this work, H_2S detection using a two-dimensional MoS_2 sensor in addition to the detection of well-known gases (e.g. NH_3, NO_2, H_2 and volatile organic compounds) is reported. The H_2S response is lower than the NH_3 response on the MoS_2 sensor, confirming that the MoS_2 sensor has lower charge transfer for the detection of H_2S than NH_3 gas. Compared to an undecorated MoS_2 sensor, the Pt NP-decorated MoS_2 sensor detected NH_3 and H_2S gas with high sensitivity down to 600 ppb and 5 ppm, respectively. In addition, NH_3 detection experiments were conducted at concentrations of 600 ppb or less in order to determine the LOD of the Pt-decorated MoS_2 sensor for NH_3 gas.

2. Material and methods

2.1. MOCVD growth of two-dimensional MoS_2 monolayer film with bilayer islands

As previously reported [35], the two-dimensional MoS_2 film was grown using MOCVD. The MoS_2 film was grown by a showerhead-type reactor using $Mo(CO)_6$ (better than 99.9% purity, Sigma-Aldrich),

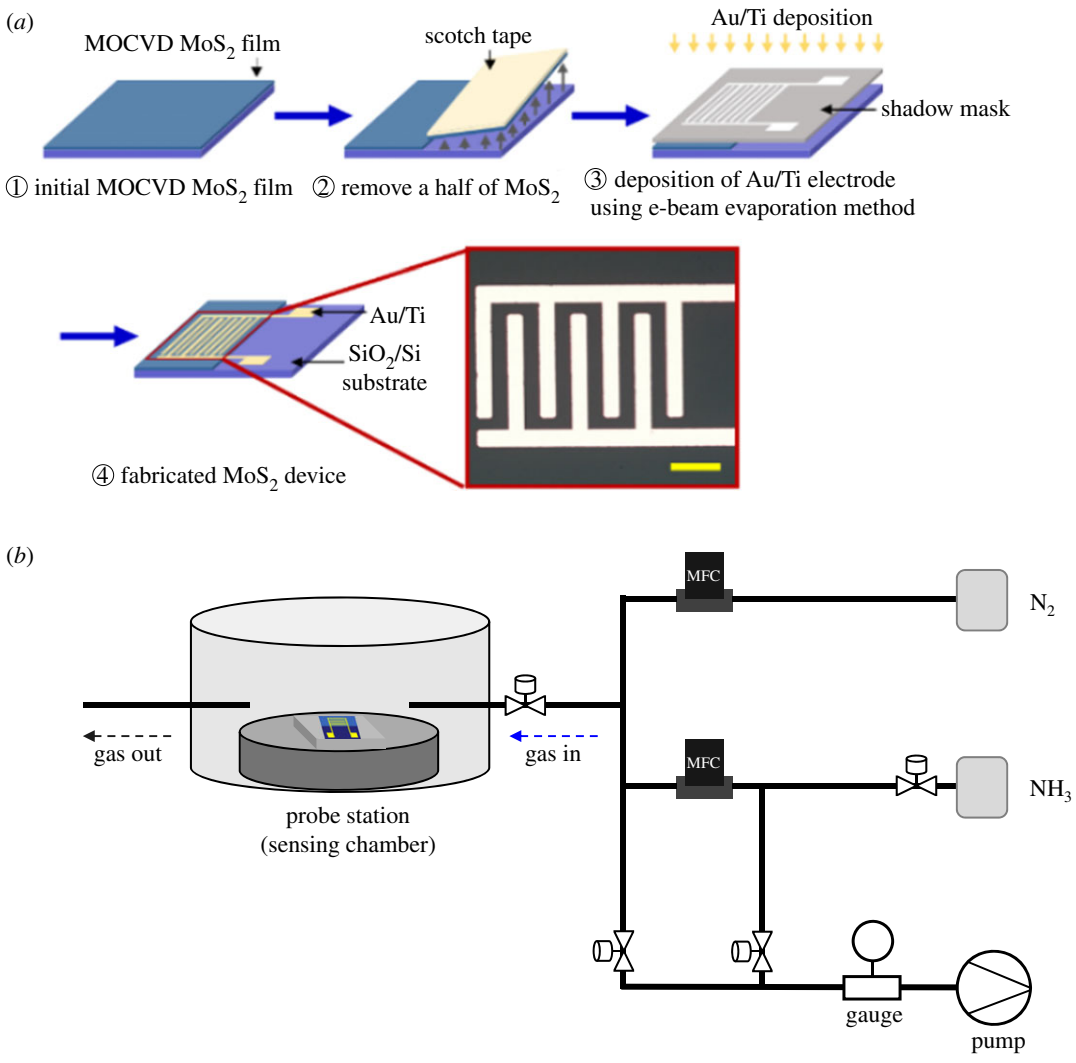

Figure 1. (*a*) Schematic illustration of the fabrication of MoS_2 gas sensor and optical image of interdigitated electrode on the MoS_2. The scale bar is 50 µm. (*b*) Schematic illustration of the gas-sensing system.

high-purity H_2 (99.999%), Ar (99.999%) and H_2S (99.9%) with an operating temperature of 400°C. A p-type silicon wafer (1–10 Ω cm) with 300 nm silicon dioxide was used as the substrate for growth. The piranha solution ($H_2SO_4 : H_2O_2 = 3 : 1$) was used for pretreatment to passivate dangling bonds [35] and make a hydrophilic substrate, resulting in the control of more nucleation sites on the substrate; the piranha treatment was performed by immersing the substrate in the piranha solution for 10 min. After immersion in the piranha solution, the substrate was thoroughly rinsed in deionized water through immersion and sonication, and it was blow-dried with high-purity N_2 (99.999%). After cleaning this, the substrate was placed on a silicon carbide-coated graphite susceptor and immediately loaded into a load-lock chamber, which was connected with the MOCVD process chamber to prevent any contamination. Subsequently, the substrate on the graphite susceptor was loaded into the process chamber to grow the two-dimensional MoS_2 film. MoS_2 film was grown using sublimed $Mo(CO)_6$ precursor vapour with high-purity H_2S, Ar and H_2 flow for high-quality MoS_2 at 300°C by the reaction between sulfur and gas with the Mo-precursor under a pressure of 5 Torr. Consequently, the fully covered monolayer MoS_2 film was synthesized with bilayer islands without empty spaces of MoS_2.

2.2. Fabrication of MoS_2-based devices and decoration with metal NPs

To prevent any contamination by chemical substances during the fabrication of the MoS_2 gas sensor, we chose a solution-free process, as shown in figure 1*a*. The MoS_2 gas sensor, which consisted of the MOCVD two-dimensional MoS_2 active channel and the interdigitated electrode, was fabricated using the e-beam evaporation method with a stencil mask. To use the MoS_2 as the active material of the gas

sensor, half of the MoS_2 film was removed by the scotch-tape method. The interdigitated electrode was patterned on the remaining MoS_2 film using the e-beam evaporation method and a stencil mask with the interdigitated pattern. Additionally, the electrode pad for resistance measurement was patterned on Si with SiO_2 where the MoS_2 was removed. The interdigitated electrode region was made from 5 nm Ti and 50 nm Au using an e-beam evaporation method under a pressure of approximately 10^{-7} Torr. Figure 1*a* also shows an optical image of the active channel (MoS_2 film, 70 µm in width) and the interdigitated Au/Ti electrode of the MoS_2 gas sensor. The active channel material detects gas molecules, and the interdigitated electrode collects charge. In this work, two MoS_2-based devices (one decorated with Pt NPs and one without Pt NPs) were made to investigate the effect of Pt NP decoration. The e-beam evaporation method was used to randomly distribute Pt NPs on the MoS_2. The Pt NPs (approx. 1 nm in thickness) were monitored with a crystal thickness sensor of e-beam evaporation under a pressure of approximately 10^{-7} Torr.

2.3. Gas-sensing experiments

A gas-sensing system that allows the users to customize experimental conditions according to their need was set up, as shown in figure 1*b*. The system consisted of analyte gas (NH_3 and H_2S), dilution (or purging) gas (N_2), a pneumatic valve for opening/closing gas flow, a mass flow controller for regulating analyte gas and dilution gas, a sensing chamber for the gas detection process and a rotary pump for purging the atmosphere after gas-sensing measurements. The gas-sensing experiments were conducted under analyte gas (NH_3 or H_2S) diluted with N_2 in a sensing chamber, and the concentration of analyte gas was controlled by modulating the flow rate of analyte gas and N_2 dilution gas. The fabricated MoS_2 gas sensor was placed in the sensing chamber for gas detection. After loading one of the MoS_2 gas sensors (i.e. bare MoS_2 or Pt-decorated MoS_2), the gas-sensing system was sufficiently stabilized under N_2 gas in the chamber and then the gas-sensing experiments were repeatedly performed by automatically controlling the purging step and analysis step for 10 and 5 min, respectively. The experiments were done with analyte concentrations of 600 ppb and 1, 2.5, 5, 15, 30 and 70 ppm. To measure the LOD of NH_3 gas for the Pt-decorated MoS_2 sensor, the experiments were done with concentrations of 130 ppb. The resistance value of the MoS_2 sensor was measured with a Keysight B2985A high-resistance meter. Because the MoS_2 gas sensor has excellent gas-sensing characteristics at high operating temperatures and RT, all experiments were performed at RT under ambient pressure.

3. Results and discussion

To examine the morphology and grain size of the as-grown MoS_2, the MoS_2 film was characterized using scanning electron microscopy (SEM) (Hitachi S-4800), as shown in figure 2*a–d*: figure 2*a* shows smaller monolayer MoS_2 clusters (growth time: 1 h), figure 2*b* shows larger monolayer MoS_2 clusters with a little bit of space (growth time: 2 h) and figure 2*c* shows monolayer MoS_2 with bilayer islands (growth time: 3 h), which were obtained by controlling coverage using the growth time without a change of other process conditions. As the growth time increased, the coalescence of these monolayer islands led to a fully covered MoS_2 film. Under a highly strong sulfiding condition, the layer atoms are more strongly attracted to the substrate than to themselves, thereby accelerating two-dimensional growth. [35] Many small nucleation sites of MoS_2 were made on the SiO_2/Si substrate by pretreatment with the piranha solution, as shown in figure 2*a*,*b*. Triangular monolayer MoS_2 clusters with S-edge termination are more stable, and figure 2*a*,*b* shows the initially grown triangular MoS_2 monolayer islands on the SiO_2/Si substrate. Before the monolayer MoS_2 film had fully formed, bilayer islands began to grow on the merging monolayer islands of MoS_2 on the substrate. After sufficient growth of the MoS_2, the fully formed monolayer MoS_2 film with bilayer islands was deposited after a growth time of 4 h 30 min, as shown in figure 2*d*. Figure 2*d* shows that a monolayer two-dimensional MoS_2 film with bilayer islands was grown using the MOCVD method. Thus, MOCVD two-dimensional MoS_2 was successfully grown at 300°C by the reaction between the sulfur and gas reaction with the Mo-precursor under the sulfiding conditions. The grain size of the bilayer islands on the fully formed monolayer film was about 100 nm. Because the adsorption of gas molecules can be attributed to the influence of the many activation sites caused by the presence of the many edges site of the bilayer islands, the fully formed monolayer MoS_2 film with bilayer islands was used as the active material of the gas sensor in this work.

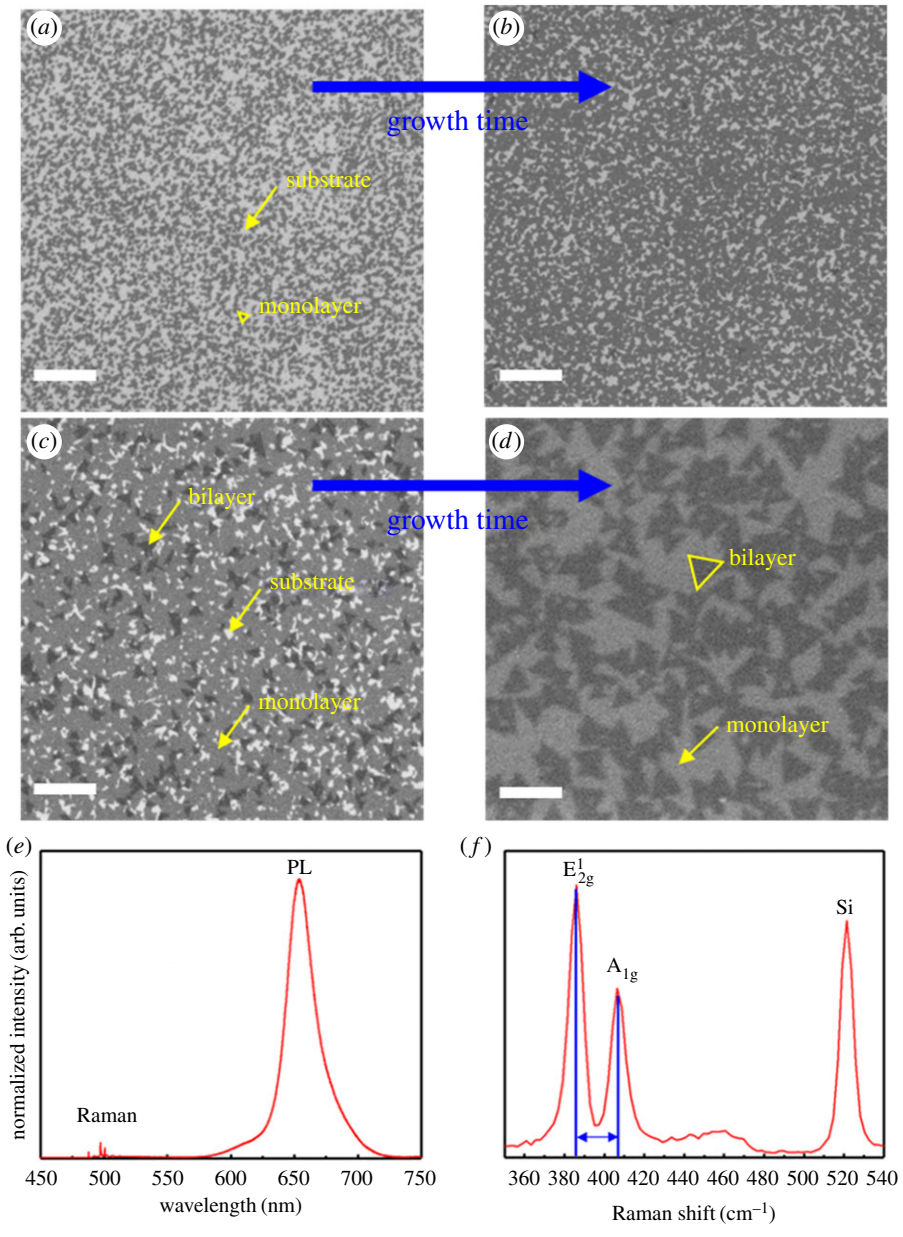

Figure 2. Characteristics of as-grown two-dimensional MoS_2. (*a*–*d*) SEM images. The scale bar is 300 nm. (*e*) Photoluminescence. (*f*) Raman spectrum.

To examine the number of the MoS_2 layers, photoluminescence and Raman spectroscopy (Renishaw inVia Raman microscope) were used. A laser with an excitation wavelength of 488 nm was used. The spectra were also normalized at the Si peak (520.7 cm^{-1}). As a result, the photoluminescence spectrum of the MoS_2 has an adsorption peak at 659 nm (1.88 eV). The Raman spectrum represents the in-plane vibration (E^1_{2g}) and the out-of-plane vibration (A_{1g}) from the MoS_2. The peak position difference between E^1_{2g} and A_{1g} was 21.81 cm^{-1}, which indicates that the MoS_2 has two layers based on the laser wavelength.

To investigate the effects of Pt NP decoration, we made two sensors: an undecorated MoS_2 sensor and a Pt NP-decorated MoS_2 sensor. Henceforth, the undecorated MoS_2 and Pt NP-decorated MoS_2 sensors will be denoted as bare MoS_2 and Pt : MoS_2, respectively. Before the gas-sensing experiments, a transmission electron microscope (TEM) (FEI Tecnai G2 F30 S-Twin) was used to characterize the morphology and structure of the as-obtained Pt : MoS_2. The decorated Pt NPs on MoS_2 were confirmed by TEM images. As shown in figure 3, a number of Pt NPs indicated by yellow circles and the TEM image clearly show small NPs with a diameter around 5 nm. The TEM image of the Pt : NP-decorated MoS_2 reveals the monolayer MoS_2 film (brightest), the triangular bilayer islands (brighter) and the Pt NPs (darker). Moreover, since Pt NPs were physically decorated by the e-beam evaporation method, the TEM image showed that the Pt NPs were randomly distributed on the MoS_2.

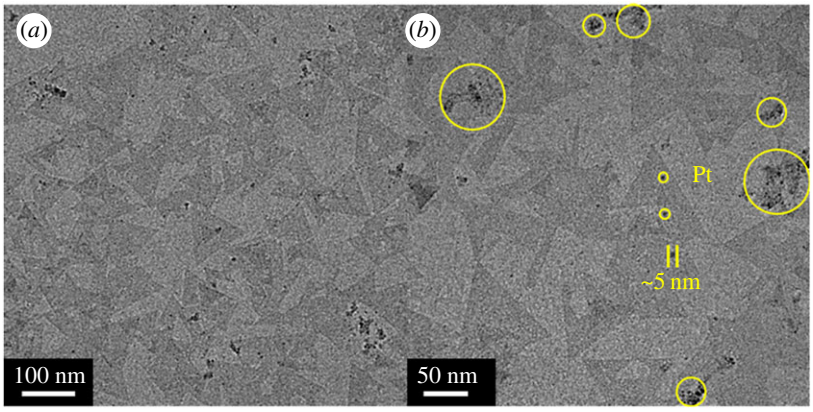

Figure 3. TEM images of the Pt : MoS_2.

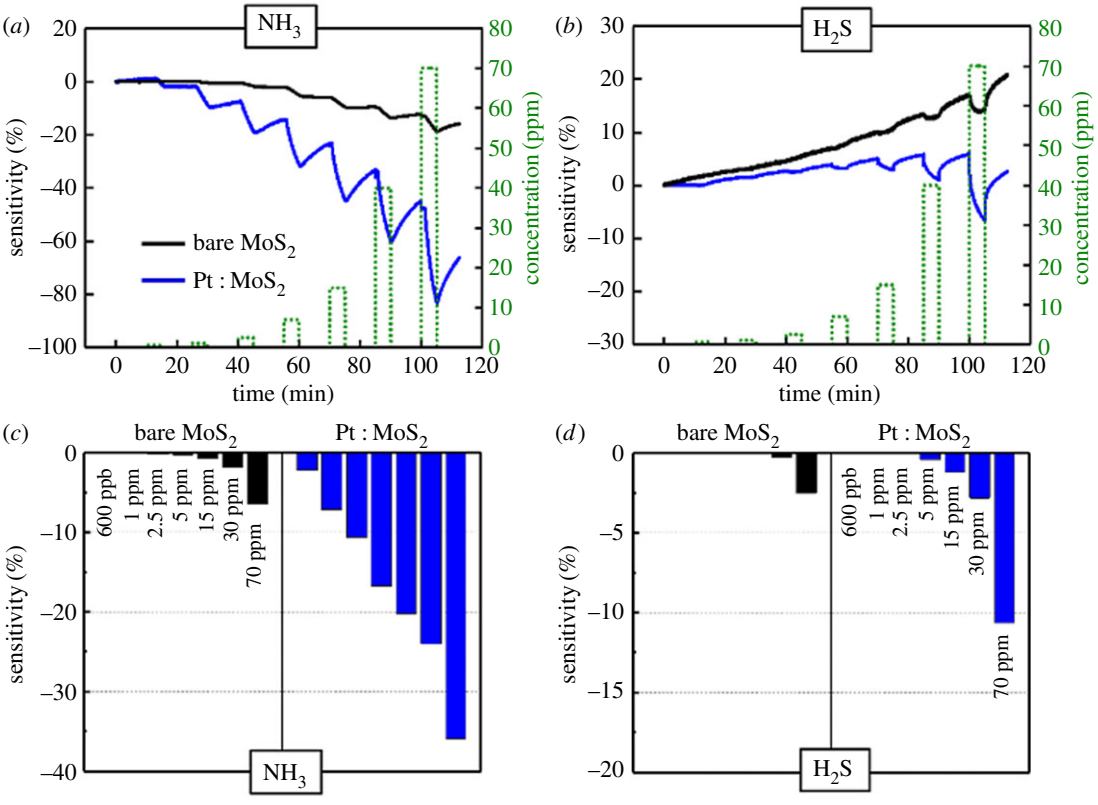

Figure 4. Gas-sensing characteristics of the MoS_2 gas sensor (*a*,*c*) Transient NH_3 or H_2S gas-sensing characteristics. (*b*,*d*) Gas sensitivity summary of NH_3 or H_2S of the bare MoS_2 and Pt : MoS_2 gas sensor.

The transient NH_3 or H_2S gas-sensing characteristics of the two MoS_2 gas sensors are shown in figure 4. With incrementally increasing concentrations (600 ppb and 1, 2.5, 5, 15, 30 and 70 ppm) of analyte gas, the gas responses of two sensors were investigated under NH_3 and H_2S gas. The sensitivity to the analyte gas was calculated using $\Delta R/R_p = (R_a - R_p)/R_p$, where R_p and R_a represent the resistances of the device under the N_2 gas (purging gas) and the analyte gas, respectively. When exposed to the NH_3 or H_2S gas, the MoS_2 sensors showed decreasing resistance (negative sensitivity). This means that both NH_3 and H_2S gas act as electron donors, transferring electrons to the conduction band of MoS_2 [15]. Thus, this leads to increased electron concentration and conductivity, and the resulting n-doping brings the Fermi level closer to the conduction band edge. Figure 4*a* shows that the LOD of NH_3 gas was as low as 2.5 ppm and the absolute sensitivity of NH_3 gas ranged from 2.5 to 70 ppm on the bare MoS_2 gas sensor at RT. Moreover, the LOD of H_2S gas was as low as 30 ppm, and the sensitivity of H_2S gas ranged from 30 to 70 ppm at RT, as shown in figure 4*b*. The two-dimensional MoS_2 gas sensor is the first film sensor to exhibit H_2S gas-sensing characteristics

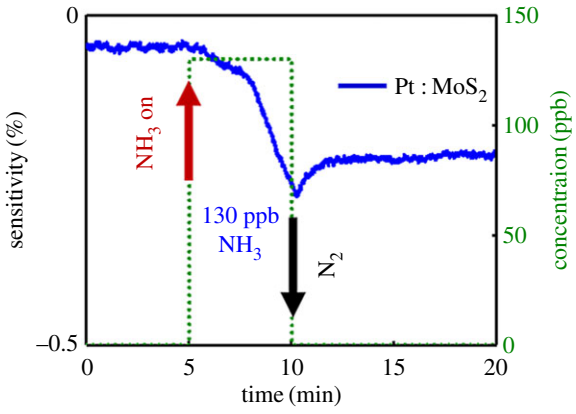

Figure 5. The Pt : NP-decorated MoS_2 gas sensor response upon exposure to 130 ppb.

Table 1. A summary of two-dimensional TMDC-based gas sensor for NH_3 or H_2S detection at RT.

no.	method of synthesis	sensing material	target gas	LOD (ppm)	operating temperature (°C)	ref.
1	CVD	MoS_2 three layer film	NH_3	5	RT	[15]
2	CVD	MoS_2 one layer film	NH_3	1	RT	[16]
3	magnetron sputtering	MoS_2nanostructure	NH_3	10	RT	[17]
4	exfoliated	$MoSe_2$ one layer	NH_3	50	RT	[18]
5	exfoliated	$MoTe_2$ few layer	NH_3	2	RT	[19]
6	exfoliated	WS_2 nanowire–nanoflake hybrid	NH_3	5	30	[20]
7	ALD	WSe_2 three layer film	NH_3	20	RT	[21]
8	MOCVD	Pt-decorated MoS_2 one layer film with bilayer islands	NH_3	0.13	RT	This work
9	exfoliated	WS_2 nanowire–nanoflake hybrid	H_2S	1	30	[20]
10	exfoliated	WSe_2 50 layer flake	H_2S	1	RT	[22]
11	MOCVD	Pt-decorated MoS_2 one layer film with bilayer islands	H_2S	5	RT	This work

(figure 4*b*). We concluded that detection of H_2S gas can be attributed to the influence of many activation sites caused by the presence of bilayer islands on the MoS_2 gas sensor. As the concentration of analyte gas (NH_3 or H_2S) increased, the absolute sensitivity of the MoS_2 sensor increased at RT (figure 4*c*,*d*). Because the bare MoS_2 gas sensor has higher sensitivity and lower LOD for NH_3 than H_2S gas sensor, it experiences a smaller charge transfer from H_2S than from NH_3. To confirm the LOD of NH_3 gas for the Pt : MoS_2 gas sensor, we performed an additional gas-sensing experiment under analyte concentrations of 600 ppb or less. This experiment demonstrates that the Pt : MoS_2 gas sensor has an LOD of NH_3 gas down to 130 ppb, as shown in figure 5. Table 1 summarizes the gas-sensing characteristics of many TMDC-based gas sensors for NH_3 or H_2S gas at RT. It shows that the Pt : MoS_2 gas sensor has high sensitivity and low LOD for both NH_3 and H_2S gas. Figure 6 shows a schematic of the energy band diagram of MoS_2 and Pt, where the work function (Φ_m) of Pt is approximately 5.65 eV [36] and the electron affinity (χ) of MoS_2 is approximately 4.2 eV [37]. Metal decoration is generally known to enhance sensitivity to a target gas, and Pt NPs act as a p-dopant, increasing sensitivity to gases that act as electron donors on the MoS_2 sensor. Overall, the Pt : MoS_2 sensor reduced the LOD of NH_3 and H_2S gas to 130 ppb and 5 ppm, respectively, which are far lower than those of the bare MoS_2 sensor (2.5 and 30 ppm, respectively). Specifically, the Pt : MoS_2 gas sensor exhibited 5.58× improved NH_3 sensitivity under a concentration of 70 ppm, and the H_2S

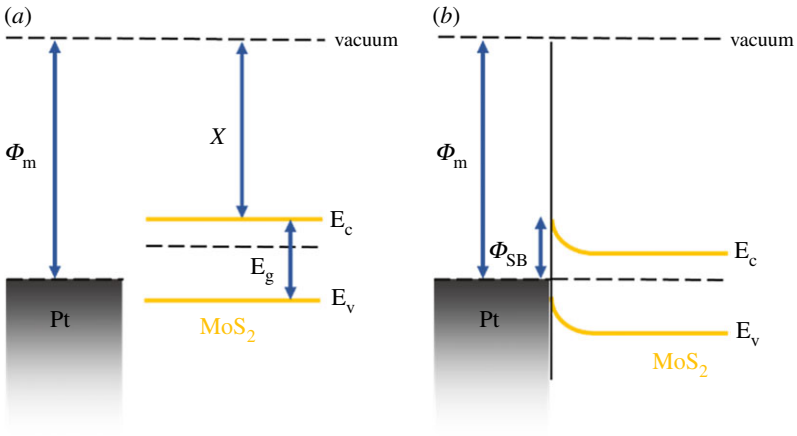

Figure 6. Pt : MoS_2 energy diagram. (*a*) Before contact. (*b*) After contact. The χ is the electron affinity of MoS_2. The Φ_m is the work function of Pt metal.

sensitivity improved by 4.25× at a concentration of 70 ppm. Even though all gas-sensing experiments were performed at RT, the bare MoS_2 and Pt : MoS_2 gas sensors exhibited excellent sensing characteristics for the target gases (NH_3 and H_2S).

4. Conclusion

In summary, Pt NPs were decorated on MOCVD two-dimensional MoS_2 to obtain high sensitivity and low LOD for NH_3 and H_2S gases. The electronic properties of MoS_2 were tuned through decoration with Pt NPs, improving the sensitivity and lowering the LOD of the gas sensor for the target gases. The Pt NPs act as a p-dopant, depleting the electron carriers of the MoS_2 film, thereby improving the sensitivity to NH_3 and H_2S gas by 5.58× and 4.25×, respectively, compared to the bare MoS_2 gas sensors under concentrations of 70 ppm. The Pt : MoS_2 gas sensor exhibited LODs of 130 ppb and 5 ppm for NH_3 and H_2S gas, respectively, which are far lower than those for the bare MoS_2 gas sensor (2.5 and 30 ppm, respectively). Even though all gas-sensing experiments were carried out at RT, the MoS_2-based gas sensors showed excellent gas-sensing characteristics. Therefore, functionalization using metal decoration on a two-dimensional gas sensor can improve the sensitivity and LOD for a specific gas by modulating the electronic properties of the two-dimensional material. This strategy opens an avenue for effective toxic gas detection with two-dimensional gas sensors.

Data accessibility. This article does not contain any additional data and all data are provided in the main text.

Authors' contributions. J.P. and J.M. conceived the study. J.P. designed and performed the calculations, and wrote the manuscript. J.-S.S. and S.-W.K. analysed the data. All the authors discussed the results, helped edit the manuscript and gave their final approval for publication.

Competing interests. The authors declare no competing interests.

Funding. This work was supported by the Technology Innovation Program (project no. 10062161, Direct low-temperature synthesis of two-dimensional materials and heterostructure on flexible substrate for next-generation high-mobility electronic devices) funded by the Ministry of Trade, Industry, and Energy (MOTIE, Korea) and development of advanced ultra-thin measurement standard technology, funded by Korea Research Institute of Standards and Science (KRISS-2018-GP2018-0012).

Acknowledgements. We thank the referees for their useful and insightful comments.

References

1. Fine GF, Cavanagh LM, Afonja A, Binions R. 2010 Metal oxide semi-conductor gas sensors in environmental monitoring. *Sensors* **10**, 5469–5502. (doi:10.3390/s100605469)
2. Sarkar D, Liu W, Xie X, Anselmo AC, Mitragotri S, Banerjee K. 2014 MoS_2 field-effect transistor for next-generation label-free biosensors. *ACS Nano* **8**, 3992–4003. (doi:10.1021/nn5009148)
3. Li H *et al.* 2012 Fabrication of single- and multilayer MoS_2 film-based field-effect transistors for sensing NO at room temperature. *Small* **8**, 63–67. (doi:10.1002/smll.201101016)
4. Perkins FK, Friedman AL, Cobas E, Campbell PM, Jernigan GG, Jonker BT. 2013 Chemical vapor sensing with monolayer MoS_2. *Nano Lett.* **13**, 668–673. (doi:10.1021/nl3043079)
5. Geim AK, Novoselov KS. 2007 The rise of graphene. *Nat. Mater.* **6**, 183–191. (doi:10.1038/nmat1849)
6. Johnson JL, Behnam A, Pearton SJ, Ural A. 2010 Hydrogen sensing using Pd-functionalized multi-layer graphene nanoribbon networks. *Adv. Mater.* **22**, 4877–4880. (doi:10.1002/adma.201001798)

7. Rumyantsev S, Liu G, Shur MS, Potyrailo RA, Balandin AA. 2012 Selective gas sensing with a single pristine graphene transistor. *Nano Lett.* **12**, 2294–2298. (doi:10.1021/nl3001293)
8. Novoselov KS, Jiang D, Schedin F, Booth TJ, Khotkevich VV, Morozov SV, Geim AK. 2005 Two-dimensional atomic crystals. *Proc. Natl Acad. Sci. USA* **102**, 10 451–10 453. (doi:10.1073/pnas.0502848102)
9. Radisavljevic B, Radenovic A, Brivio J, Giacometti V, Kis A. 2011 Single-layer MoS_2 transistors. *Nat. Nanotechnol.* **6**, 147–150. (doi:10.1038/nnano.2010.279)
10. Mak KF, Lee C, Hone J, Shan J, Heinz TF. 2010 Atomically thin MoS_2: a new direct-gap semiconductor. *Phys. Rev. Lett.* **105**, 136805. (doi:10.1103/PhysRevLett.105.136805)
11. Fang H, Tosun M, Seol G, Chang TC, Takei K, Guo J, Javey A. 2013 Degenerate n-doping of few-layer transition metal dichalcogenides by potassium. *Nano Lett.* **13**, 1991–1995. (doi:10.1021/nl400044m)
12. Liu W, Kang J, Sarkar D, Khatami Y, Jena D, Banerjee K. 2013 Role of metal contacts in designing high-performance monolayer n-type WSe_2 field effect transistors. *Nano Lett.* **13**, 1983–1990. (doi.10.1021/nl304777e)
13. Shi Y, Huang J-K, Jin L, Hsu Y-T, Yu SF, Li L-J, Yang HY. 2013 Selective decoration of Au nanoparticles on monolayer MoS_2 single crystals. *Sci. Rep.* **3**, 1839. (doi:10.1038/srep01839)
14. Liu H, Neal AT, Zhu Z, Luo Z, Xu X, Tománek D, Ye PD. 2014 Phosphorene: an unexplored two-dimensional semiconductor with a high hole mobility. *ACS Nano* **8**, 4033–4041. (doi:10.1021/nn501226z)
15. Cho B *et al.* 2015 Charge-transfer-based gas sensing using atomic-layer MoS_2. *Sci. Rep.* **5**, 8052. (doi:10.1038/srep08052)
16. Liu B, Chen L, Liu G, Abbas AN, Fathi M, Zhou C. 2014 High-performance chemical sensing using Schottky-contacted chemical vapor deposition grown monolayer MoS_2 transistors. *ACS Nano* **8**, 5304–5314 (doi:10.1021/nn5015215)
17. Sharma S, Kumar A, Kaur D. 2018 Room temperature ammonia gas sensing properties of MoS_2 nanostructured thin film. *AIP Conf. Proc.* **1953**, 030261. (doi.10.1063/1.5032596)
18. Late DJ, Doneux T, Bougouma M. 2014 Single-layer $MoSe_2$ based NH_3 gas sensor. *Appl. Phys. Lett.* **105**, 233103. (doi:10.1063/1.4903358)
19. Feng Z *et al.* 2017 Highly sensitive $MoTe_2$ chemical sensor with fast recovery rate through gate biasing. *two-dimensional Mater.* **4**, 025018. (doi:10.1088/2053-1583/aa57fe)
20. Asres GA *et al.* 2018 Ultrasensitive H_2S gas sensors based on p-type WS2 hybrid materials. *Nano Res.* **11**, 4215–4224. (doi:10.1007/s12274-018-2009-9)
21. Ko KY, Park K, Lee S, Kim Y, Woo WJ, Kim D, Song J-G, Park J, Kim H. 2018 Recovery improvement for large-area tungsten diselenide gas sensor. *ACS Appl. Mater. Interfaces* **11**, 4214–4224.
22. Hong Y, Kang Y, Cho I-T, Shin J, Wu M, Lee J-H. 2017 Gas-sensing characteristics of exfoliated WSe_2 field-effect transistors. *J. Nanosci. Nanotechnol.* **17**, 3151–3154. (doi:10.1166/jnn.2017.14039)
23. Mubeen S, Zhang T, Yoo B, Deshusses MA, Myung NV. 2007 Palladium nanoparticles decorated single-walled carbon nanotube hydrogen sensor. *J. Phys. Chem. C* **111**, 6321–6327. (doi:10.1021/jp067716m)
24. Zhang Y, Xu J, Xu P, Zhu Y, Chen X, Yu W. 2010 Decoration of ZnO nanowires with Pt nanoparticles and their improved gas sensing and photocatalytic performance. *Nanotechnology* **21**, 285501. (doi:10.1088/0957-4484/21/28/285501)
25. Cho B *et al.* 2015 Metal decoration effects on the gas-sensing properties of two-dimensional hybrid-structures on flexible substrates. *Sensors* **15**, 24 903–24 913. (doi:10.3390/s151024903)
26. Cho B *et al.* 2014 Graphene-based gas sensor: metal decoration effect and application to a flexible device. *J. Mater. Chem. C* **2**, 5280–5285. (doi:10.1039/C4TC00510D)
27. Sarkar D, Xie X, Kang J, Zhang H, Liu W, Navarrete J, Moskovits M, Banerjee K. 2015 Functionalization of transition metal dichalcogenides with metallic nanoparticles: implications for doping and gas-sensing. *Nano Lett.* **15**, 2852–2862. (doi:10.1021/nl504454u)
28. Chang J, Larentis S, Tutuc E, Register LF, Banerjee SK. 2014 Atomistic simulation of the electronic states of adatoms in monolayer MoS_2. *Appl. Phys. Lett.* **104**, 141603. (doi:10.1063/1.4870767)
29. Rastogi P, Kumar S, Bhowmick S, Agarwal A, Chauhan YS. 2014 Doping strategies for monolayer MoS_2 via surface adsorption: a systematic study. *J. Phys. Chem. C* **118**, 30 309–30 314. (doi:10.1021/jp510662n)
30. Kuru C, Choi C, Kargar A, Choi D, Kim YJ, Liu CH, Yavuz S, Jin S. 2015 MoS_2 nanosheet-Pd nanoparticle composite for highly sensitive room temperature detection of hydrogen. *Adv. Sci.* **2**, 1500004. (doi:10.1002/advs.201500004)
31. Zhao PX, Tang Y, Mao J, Chen YX, Song H, Wang JW, Song Y, Liang YQ, Zhang XM. 2016 One-dimensional MoS_2-decorated TiO_2 nanotube gas sensors for efficient alcohol sensing. *J. Alloys Compd.* **614**, 252–258. (doi.10.1016/j.jallcom.2016.03.029)
32. Xu S, Sun F, Yang S, Pan Z, Long J, Gu F. 2015 Fabrication of SnO_2-reduced graphite oxide monolayer-ordered porous film gas sensor with tunable sensitivity through ultra-violet light irradiation. *Sci. Rep.* **5**, 8939. (doi:10.1038/srep08939)
33. Cho S-Y, Kim SJ, Lee Y, Kim J-S, Jung W-B, Yoo H-W, Kim J, Jung H-T. 2015 Highly enhanced gas adsorption properties in vertically aligned MoS_2 layers. *ACS Nano* **9**, 9314–9321. (doi:10.1021/acsnano.5b04504)
34. Hassan Hu, Mun J, Kang BS, Song JY, Kim T, Kang S-W. 2016 Sensor based on chemical vapour deposition-grown molybdenum disulphide for gas sensing application. *RSC Adv.* **6**, 75839. (doi:10.1039/C6RA10132A)
35. Mun J, Kim Y, Kang I-S, Lim SK, Lee SJ, Kim JW, Park HM, Kim T, Kang S-W. 2016 Low-temperature growth of layered molybdenum disulphide with controlled clusters. *Sci. Rep.* **6**, 21854. (doi:10.1038/srep21854)
36. Michaelson HB. 1977 The work function of the elements and its periodicity. *J. Appl. Phys.* **48**, 4729. (doi:10.1063/1.323539)
37. Gong C, Zhang H, Wang W, Colombo L, Wallace RM, Cho K. 2015 Band alignment of two-dimensional transition metal dichalcogenides: application in tunnel field effect transistors. *Appl. Phys. Lett.* **107**, 139904. (doi:10.1063/1.4817409)